

Multilink Communities of Multiplex Networks

Raúl J. Mondragón,¹ Jacopo Iacovacci,² and Ginestra Bianconi²

¹ *School of Electronic Engineering and Computer Science,
Queen Mary University of London E1 4NS, United Kingdom*

² *School of Mathematical Sciences, Queen Mary University of London E1 4NS, United Kingdom*

Multiplex networks describe a large number of complex social, biological and transportation networks where a set of nodes is connected by links of different nature and connotation. Here we uncover the rich community structure of multiplex networks by associating a community to each multilink where the multilinks characterize the connections existing between any two nodes of the multiplex network. Our community detection method reveals the rich interplay between the mesoscale structure of the multiplex networks and their multiplexity. For instance some nodes can belong to many layers and few communities while others can belong to few layers but many communities. Moreover the multilink communities can be formed by a different number of relevant layers. These results point out that mesoscopically there can be large differences in the compressibility of multiplex networks.

The current Big Data explosion requires the development of new algorithms and theoretical methods to extract information from large datasets. Often in this context, it is advantageous to combine information coming from different sources and to represent the data by a multiplex network [1–5]. A multiplex network is formed by a set of nodes connected in different layers by links indicating interactions of different types. Multiplex networks are ubiquitous spanning from complex infrastructure networks [4, 6, 7], to social [8–11] biological [8, 12] and transportation networks [13, 14]. For instance, individuals can be related by different type of social ties, neurons can interact through chemical synapses and electrical gap junctions, and two locations can be connected by different means of transportation.

A multiplex network tends to have a richer structure than single networks and this richness is reflected in its communities [9, 10, 15–17]. The communities of a multiplex network cannot be obtained by considering its layers individually. Some communities might exist only in one layer, other communities can overlap on many layers and finally there are communities that only exist when considering the whole structure of the multiplex network. Several algorithms [9, 18–22] have been recently proposed to detect multilayer communities. These include methods based on multilayer modularity optimization [9, 20], diffusion properties on multilayer networks [18, 21] and consensus clustering [22]. All these techniques are node-based community detection methods where each node or each replica-node (realization of a node in a given layer) is classified in one community. Interestingly in the framework of single-layer community detection [23, 24] it has been observed that link-based community detection methods [25, 26] can be very fruitful to describe the mesoscale organization of networks when nodes belong to several communities at the same time [27]. The need to extend the link communities to multiplex network is rather pressing. For instance if we consider individuals interacting through different on-line social network platforms, say Twitter and Facebook, it might be misleading to think that an individual or an account (a Twitter or Facebook account) might belong just to a single commu-

nity. In fact, influential Twitter or Facebook accounts tend to reach more than one community of the same on-line platform.

In simple networks any two nodes can be either connected or not connected by a link, in multiplex network any two nodes can be connected in multiple ways. We say that two nodes are connected via a *multilink* [3, 11], where the multilink describes the pattern of connections between two nodes. In this work we propose a multilink community detection method for multiplex networks which extends link communities to the multiplex network framework. Our community detection method is based on the similarity of incident multilinks. In order to reduce unnecessary layer-information, the similarity between two multilinks is measured by comparing the local structure of the multiplex against a local, maximum entropy null model. To avoid introducing bias via the null model, the null model describes our state of knowledge of the multiplex in a way that is maximally noncommittal to the layered structure.

Here we show that using the proposed multilink community detection method not only we are able to extract relevant information on the mesoscale structure of multiplex networks, but also we can contribute to the scientific debate about the compressibility of the multiplex network structures. Recent research on multiplex networks questions whether it is opportune to aggregate or disaggregate their layers. Aggregation of layers could be useful for removing redundant information. De Domenico et al. [28], have shown that for the vast majority of multiplex networks there is trade-off between the information content and the minimization of their total number of layers. The case of disaggregating a single network to a multi-layer network has been considered by Vales-Catala et al. in Ref. [29]. According to their results some single networks are better represented as multiplex networks because they are effectively the result of a blind multiplex network aggregation procedure. Finally, Peixoto [30], using a statistical inference approach, has revealed that there is no clear answer, the benefits of the aggregation or disaggregation of the layers are dependent on the system under study.

Here we show that actually the optimal answer to the question whether it is more appropriate to aggregate or disaggregate a general multiplex network might not be global but mesoscale. Our analysis of social, biological and transportation networks reveals that in multiplex networks there is a very rich interplay between their mesoscale organization and their multiplexity. Multilink communities can include connections of only one layer or of multiple layers. Additionally we observe that not always the layer activity (in how many layers a node is connected) correlates with the community activity (in how many communities a node can be found). For example there can be nodes that are connected in many layers (high layer activity) but belong only to few multilink communities (low community activity) and nodes belonging to few layers (low layer activity) but belonging to many multilink communities (high community activity). The first possibility suggests that mesoscopically the network could be compressed while the second possibility suggests that mesoscopically the network could be expanded into many layers making a case for a definition of a mesoscale compressibility of the multiplex network.

RESULTS

Multiplex network

Let us consider a multiplex network formed by N nodes and M layers $\alpha = 1, 2, \dots, M$. The multiplex network is the set of M networks $\vec{G} = \{G^{[1]}, G^{[2]}, \dots, G^{[\alpha]}, \dots, G^{[M]}\}$ where each network $G^{[\alpha]} = \{V, E^{[\alpha]}\}$ is formed by the same set of N nodes $V = \{i; i = 1, 2, \dots, N\}$ and by the set of links $E^{[\alpha]}$ which describe the connections in layer α . We assume that all these networks are undirected and we represent each layer $\alpha = 1, 2, \dots, M$ by the adjacency matrix $\mathbf{a}^{[\alpha]}$. The whole multiplex network can be expressed via its multilinks [3, 11]. Every pair of nodes (i, j) is connected by a multilink

$$\vec{m}_{ij} = (m_{ij}^{[1]}, m_{ij}^{[2]}, \dots, m_{ij}^{[\alpha]} \dots m_{ij}^{[M]}), \quad (1)$$

with $m_{ij}^{[\alpha]} = a_{ij}^{[\alpha]}$ indicating in which layers of the multiplex network the two nodes are connected. Whenever node i and node j are connected at least in one layer, i.e. $\vec{m} \neq \vec{0}$, we say that they are connected by a non-trivial multilink. To decide if a non-trivial multilink exist, it is convenient to construct the aggregated network \hat{G} formed by the N nodes of the multiplex. The adjacency matrix \mathbf{A} of the aggregated network \hat{G} has elements

$$A_{ij} = \theta \left(\sum_{\alpha=1}^M a_{ij}^{[\alpha]} \right), \quad (2)$$

where $\theta(x)$ is the step function $\theta(x) = 1$ if $x > 0$ and $\theta(x) = 0$ if $x \leq 0$. We indicate with $L = \sum_{i < j} A_{ij}$

the total number of links of the aggregated network, or equivalently the number of non-trivial multilinks.

In a multiplex network the nodes might not be connected in each layer. The number of layers in which a node is connected (or active) is called the *node activity* [8, 31] and reveals relevant coarse grained information about the node.

Multilink similarity

In the context of single networks several community detection methods use hierarchical clustering applied either to a similarity matrix between nodes [32] or between links [25, 26]. Here we construct a hierarchical clustering of multiplex networks based on a measure of similarity between incident multilinks. By defining the similarity between multilinks here we generalize the link communities previously defined for single layers [25, 26] to multiplex networks.

In a similar spirit to the use of the modularity function for detecting node communities [33], the similarity between incident multilinks is evaluated by comparing simultaneously the cohesiveness and the multiplexity of their neighbourhood to a maximum entropy null model.

To every pair of multilinks connecting nodes i and k and nodes j and s we assign the similarity $S_{ik,j,s}$. The similarity $S_{ik,j,s}$ is non-zero only between incident multilinks (i.e. for $s = k$) and is a function of two parameters: ϵ and z . The parameter $\epsilon \in (0, 1)$ can be tuned depending on the role that we want to assign to the composition of the two incident multilinks with respect to their local neighborhood. The additional parameter $z \in (0, 1)$ evaluates the role of multiplexity and represent the cost we want to attribute to incident multilinks of different composition.

Specifically the non-zero similarities $S_{ik,j,k}$ are given by

$$S_{ik,j,k} = \epsilon \sigma_{ijk} + (1 - \epsilon) \sigma_{ij \setminus k}. \quad (3)$$

where σ_{ijk} evaluates the contribution of the two incident multilinks while $\sigma_{ij \setminus k}$, evaluates instead the contribution due to the existence of other multilinks, joining node i and node j directly or by paths of length two excluding node k . The parameter $\epsilon \in (0, 1)$ tunes the relative importance between these two contributions. The term σ_{ijk} is expressed as

$$\sigma_{ijk} = z^{\beta_{ik,jk}}, \quad (4)$$

with

$$\beta_{ij,rs} = 1 - \frac{\sum_{\alpha=1}^M m_{ij}^{[\alpha]} m_{rs}^{[\alpha]}}{M}. \quad (5)$$

The smaller is z the larger is the ‘‘penalty’’ for having multilinks \vec{m}_{ik} and \vec{m}_{jk} with different layer composition. If the multilinks connecting nodes (i, k) and

(j, k) have not even a link in a common layer, $\beta_{ik,jk} = 1$ and $z^{\beta_{ik,jk}} = z$, indicating the maximum cost attributed to multiplexity. If, on the contrary the two multilinks have the same layer composition, then $\beta_{ik,jk} = 0$ and $z^{\beta_{ik,jk}} = 1$ indicating that we attribute no cost penalty to this configuration.

The term $\sigma_{ij \setminus k}$ includes contributions from paths of length one (\mathcal{M}_{ij}) and two ($\hat{\mathcal{M}}_{ijr}$) between node i and node j that pass through node r with $r \neq k$, i.e.

$$\sigma_{ij \setminus k} = \frac{1}{\mu} \left[\mathcal{M}_{ij} + \sum_{r \neq k} \hat{\mathcal{M}}_{ijr} \right], \quad (6)$$

where μ is a normalization constant with $\mu = \max(1, \nu)$ with

$$\nu = \min \left(\sum_{r \neq k} A_{ir}, \sum_{r \neq k} A_{jr} \right). \quad (7)$$

Similarly to the modularity measure [33], term \mathcal{M}_{ij} evaluates the significance of the observed multilink \bar{m}_{ij} against its expectation and, $\hat{\mathcal{M}}_{ijr}$ evaluates the significance of two non-trivial multilinks $\bar{m}_{ir}, \bar{m}_{jr}$ connecting respectively node i and node j to a common node $r \neq k$ against their expectations. These terms are

$$\begin{aligned} \mathcal{M}_{ij} &= (A_{ij} - p_{ij}^{\bar{m}_{ij}}) z^{\beta_{ij,ij}} \delta(A_{ij}, 1), \\ \hat{\mathcal{M}}_{ijr} &= (A_{ir} A_{jr} - p_{ir}^{\bar{m}_{ir}} p_{jr}^{\bar{m}_{jr}}) z^{\beta_{ir,jr}} \delta(A_{ir} A_{jr}, 1), \end{aligned} \quad (8)$$

where $\beta_{ij,rs}$ is given by Eq. (S-15), and $\delta(x, y)$ is the Kronecker delta (i.e. $\delta(x, y) = 1$ for $x = y$ and $\delta(x, y) = 0$ otherwise). The term $z^{\beta_{ij,rs}}$ puts a cost to the paths that are created using different layers. The expectation of multilink \bar{m}_{rs} is given by the probability $p_{rs}^{\bar{m}_{rs}}$, which is evaluated using maximum entropy ensembles preserving the degree of node i and node j in each layer α , and the multilinks $\bar{m}_{ik}, \bar{m}_{jk}$ (see Methods and SI for details).

Multilink Communities

From the $L \times L$ similarity matrix $S_{ik,jk}$, we construct a dendrogram via single linkage hierarchical clustering. The dendrogram contains information about the multiplex structure which cannot be obtained from the aggregated network. Finally the multilink communities are determined by cutting the dendrogram at a height that correspond to an optimal value of a appropriate score function.

To obtain the multilink communities we desire to use a score function that does not use any a priori assumptions about the multilink composition. To this end we have considered a score function used on single-layer link-community detection methods, i.e. the link modularity \mathcal{Q} [26] (see Method for its definition). An alternative choice could be to choose the partition density D used in

[25]. The optimal partition is defined by the maximum value of \mathcal{Q} obtained when considering all the heights in the dendrogram (see SI for typical profiles of this link modularity on real datasets).

Once every multilink is associated to a given multilink community we can assign to each node a *community activity* given by the number of communities to which its incident multilinks belong.

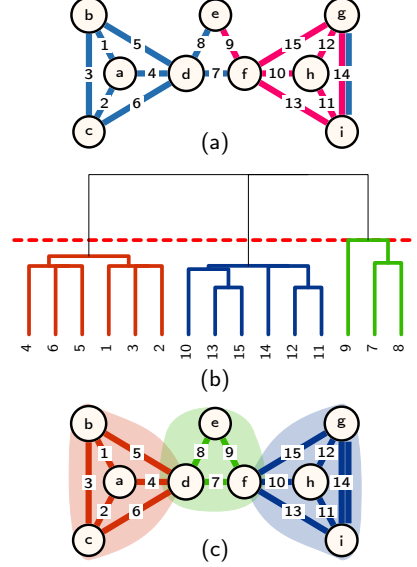


FIG. 1: (a) A simple multiplex and (b) its dendrogram obtained from the multilink similarity. The dashed red line shows the maximum link modularity used to define the link communities. Panel (c) shows the partition of the multiplex network into three communities revealing that communities can be formed by a single (community $\{a, b, c, d\}$) or multiple layers (community $\{d, e, f\}$) and that the nodes communities are independent on the node activity (node d belongs to two community and is active in one layer, node g is belongs to one community and is active in one layer). The multilink communities are detected using $\epsilon = 0.4, z = 0.6$.

DISCUSSION

A simple example

The community activity of a node resulting from the multilink community detection method is independent on its layer activity. To illustrate this property we consider the multilayer network shown in Fig. 1(a) decomposed in three multilink communities 1(c)) detected using the parameters $\epsilon = 0.4$ and $z = 0.6$. Node d is active in a single layer but belongs to two multilink communities. On the contrary node g is active in two layers but belongs to just one community.

Additionally the communities can be formed by interactions existing only in one layer or in multiple layers.

For instance the community formed by the nodes $\{e, d, f\}$ of the multiplex network shown in Fig. 1(a), only exist due to the combination of different layers in the multiplex. On the contrary the community formed by the nodes $\{a, b, c, d\}$ include only links of a single layer.

The dendrogram in Fig. 1(b) shows the hierarchical structure of the link communities of the multiplex network in Fig. 1(a) and reveals the multilayer nature of the network also in the case of this very symmetrical and clustered topology. In fact, the left and right communities of Fig. 1(c), although they play the same role in the aggregated network, have a different decomposition into multilink sub-communities. There are two factors that contribute to this difference. The right community has a multilink formed by two layers (multilink 14) which is no present in the other community. The second factor is more subtle and it would generate differences in the hierarchical structure even if the community on the right included only links existing in a single layer (see SI for details).

Florentine Families

The Florentine Families Multiplex Network [34] consist of $M = 2$ two layers, one layer describes the business dealings between $N = 16$ florentine families in the XV century, the other layer their alliances due to marriages. Fig. 2(a) shows these relationships between the families. Figure 2(b) shows the dendrogram describing the multilink communities for $\epsilon = 0.5, z = 0.6$ (see SI for the dependence of the number of clusters on ϵ and z).

The two detected single multilink communities correspond to two different scenarios (Fig. 2(c)). The multilink between the Strozzi and the Ridolfi family establish an interaction between two families which have connections between different clusters; the multilink between the Acciaiuoli and the Medici family is a leaf of the multiplex network, being the only multilink connecting the Acciaiuoli family to the rest of the multiplex network.

For each family we compare their *layer activity* and their *community activity* (Fig. 2(d)). We observe that families with high community activity are powerful brokers between different communities. Most relevantly, the Medici play a pivotal role as they are brokers between three different communities. The Barbadori and the Guadagni family have the same community activity as the Ridolfi and the Strozzi family but while the first two are connected in both layers the latter two are connected to the other families exclusively in one layer (the marriage alliances).

Multiplex Connectome of *C. elegans*

The Multiplex Connectome of *C. elegans* [35, 36] has two layers $M = 2$, the chemical synapses and the gap junctions describing the interactions between $N = 279$

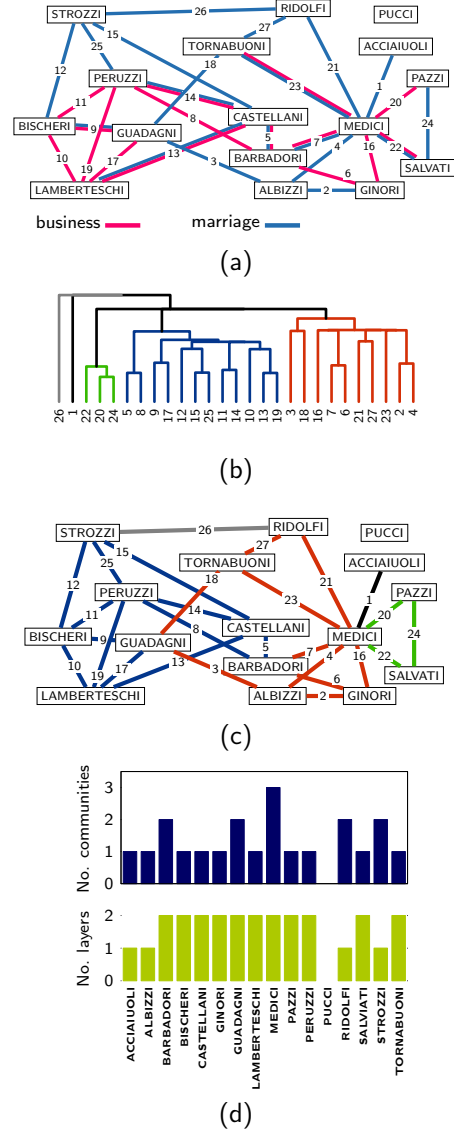


FIG. 2: (a) The Florentine Families Multiplex Network describing the business and marriage alliances of the XV century florentine families. (b) Heat map displaying the multilink similarity matrix and its relative dendrogram. (c) Partition of the Florentine Families multiplex network into five multilink communities. (d) Layer and community activity of the different families. The Medici family is characterized by achieving the maximum of the community activity. The multilink communities are detected using $\epsilon = 0.4, z = 0.6$.

neurons. As an example, we obtained the multilink communities for $\epsilon = 0.4$ and $z = 0.6$. The multiplex has 845 multilink communities of which 652 (about 77%) are made of single multilinks. The distribution of the sizes of the communities is broad. (Fig. 3(a)). The largest community is formed by 878 multilinks followed communities including 67 links and 51 links. Although there is

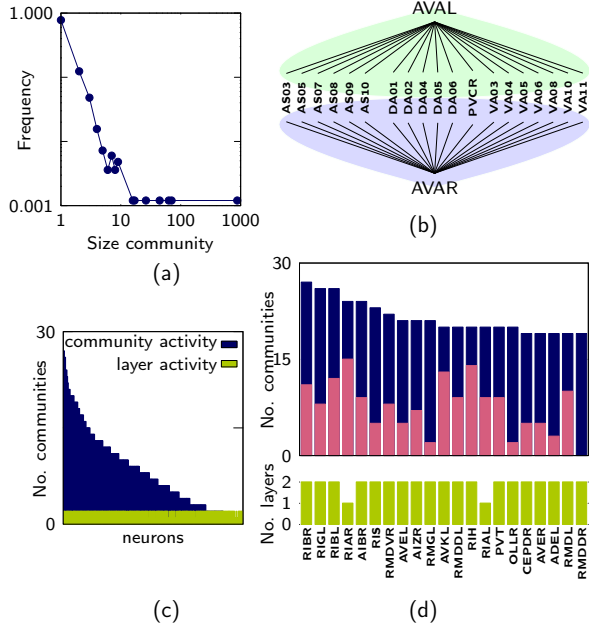


FIG. 3: (a) Distribution of the communities sizes for the Multiplex Connectome of *C. elegans*. (b) The two most similar sub-communities contained in the largest multilink community. (c) Neurons ranked in decreasing order of their community activity. (d) Layer and community activity for the top ranked neurons. (the contribution of communities with single multilinks is in pink while the contributions of communities with more than one multilink is in blue). The multilink communities are detected using $\epsilon = 0.4$, $z = 0.6$.

a large dominant community in the multiplex network, the internal structure of this community can be investigated via the dendrogram. We noticed that the ADAL and ADAR are the neurones that cluster first with some of their neighbouring neurones (Fig. 3(b)) for all values of z .

This multiplex has neurons which have large community activity (Fig. 3(c)). By ranking the neurons according to their community activity we find in the first two positions the RIBR and RIBL neurons, which are head interneurons connected via gap junctions to multiple other neuron classes, suggesting that these neurons play a role in brokering between different communities (Fig. 3(d)).

European Multiplex Air Transport Network

The European Multiplex Air Transport Network [14] comprises of $N = 417$ European airports and $M = 37$ layers corresponding to the airlines that have flight connections between these airports. The total number of multilink describing these connections is 2953. For the case that $\epsilon = 0.4$ and $z = 0.6$, our algorithm obtains 1790 multilink communities. The largest community includes

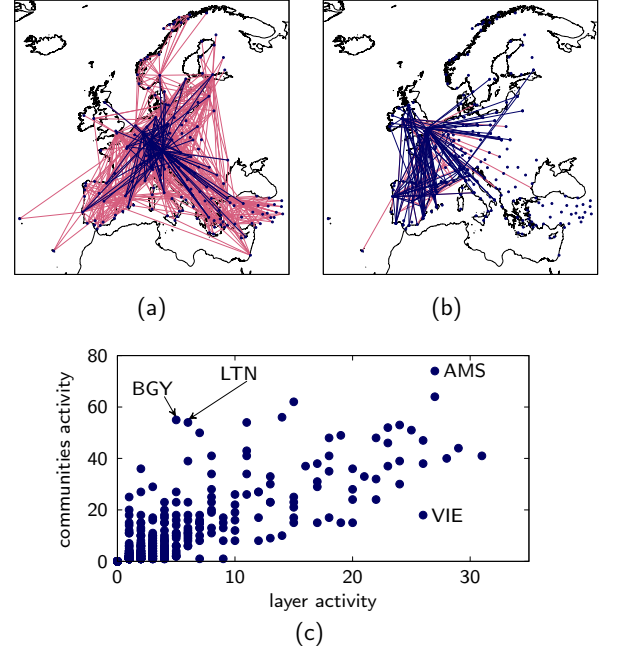


FIG. 4: (a) Largest link community of the European Multiplex Air Transportation Network. Lufthansa's flights are shown in blue, the other airlines in pink. (b) Second largest link community. Ryanair's flights are shown in blue, the other airlines in pink. (c) Community vs. layer activity of the EU airports. While the layer activity appears to have a positive correlation with the community activity, large difference in community activity can be observed between airports with large layer activity (compare for instance Amsterdam (AMS) and Vienna (VIE)). The multilink communities are detected using $\epsilon = 0.4$, $z = 0.6$.

723 nodes, about 24% of the total number of multilinks. The smallest communities are made of single multilinks and there are 1696 of them, about 57% of the multilinks.

We observe that the main communities have very different composition in term of single layers. Figure 4(a)-(b) shows the two largest communities. All the airlines (layers) contribute to the structure of the largest community (Fig. 4(a)). The second largest community has a very different structure, only few airlines contribute to this community.

When comparing the airports and their community activity, we observe (Fig. 4(c)) that while large layer activity, an airport serving multiple airline companies, seems to be correlated to high community activity, there is a significant variability in the community of airports that are active in many layers. For example Vienna (VIE) and Amsterdam (AMS) have a comparable layer activity but very different community activity. Similarly there are airports with small layer activity but significant community activity, for example Luton (LTN) and Bergamo (BGY) airports. This indicates that the airports might adopt different strategies to broker between different commu-

nities. These strategies might involve serving flights of many airline companies or serving flights of relatively fewer airline companies.

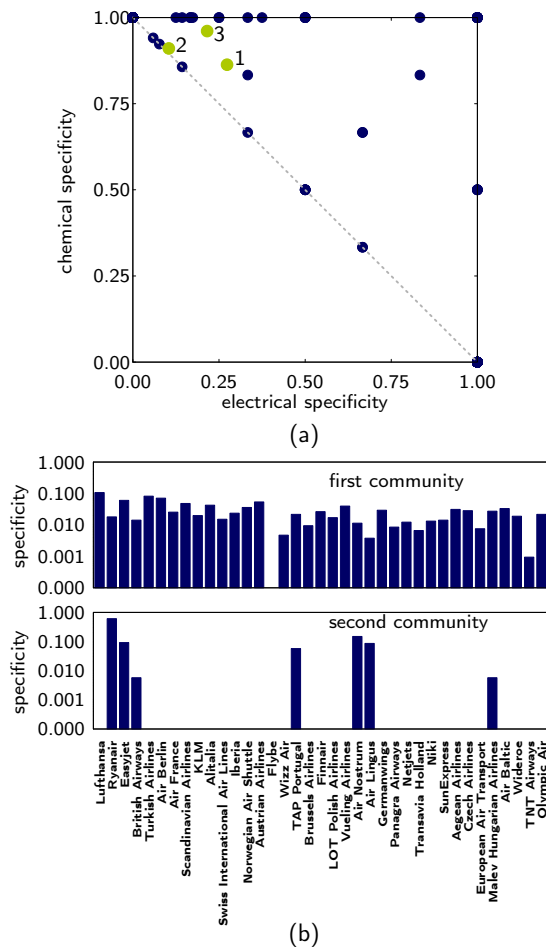


FIG. 5: (a) Specificity for the communities in the Multiplex Connectome of *C. elegans*. (b) Specificity for the first and second largest communities for the European Air Transportation Network. Both panels indicate a large variability in the layer composition of different communities. The multilink communities are detected using $\epsilon = 0.4$, $z = 0.6$.

Composition of the multilink communities

To investigate whether the communities are formed exclusively by links of a single layer or include links of several layers we introduce the *layer specificity* $x_c^{[\alpha]}$ which is the fraction of multilinks in a community c which include a link in layer α . Therefore $x_c^{[\alpha]} = 1$ indicates that all the multilinks of a community include a link in layer α , while $x_c^{[\alpha]} = 0$ indicates that the community does not include any link in layer α . Note that since a single multilink can include links of different layers, the sum of the layer

specificity $x_c^{[\alpha]}$ for community c in general do not add to one.

In the Multiplex Connectome of *C. elegans* we observe that many communities are exclusively formed by one type of multilink, however, the three largest communities have a multiplex nature as they include different types of multilinks (see Fig. 5(a) where the larger communities are indicated by the labels 1, 2, 3 in order of decreasing size).

In the European Multiplex Air Transportation Network, the largest community, apart from Flybe, contains flights from all other airlines (Fig 5(b)). The largest contribution comes from Lufthansa with an specificity of 0.10 followed by Turkish Airlines with 0.07 specificity. The second largest community has a different structure, in this case only seven airlines contribute to the community, the largest contribution is from Ryanair with a specificity of 0.60. In this multiplex, low-cost airlines like Ryanair, Easyjet and Wideroe have high specificity (often equal to 1) in many communities. However these airlines rarely have high specificity in the same community. This is a consequence of the competition between low-cost airline companies as they tend to differentiate each other by having unique flights to some destinations.

CONCLUSIONS

Our method reveal the richness of multiplex networks at their mesoscale structure. This is achieved by associating to each pair of incident multilinks a similarity measure based on the comparison of the local connectivity of two multilinks against a null model. Our intrinsically multiplex community detection method allow us to associate to each node multiple communities independently on its layer activity. Specifically we can have nodes active exclusively in one layer and belonging to multiple communities or active in many layers but belonging only to few communities. The proposed method is here applied to several real datasets revealing that the mesoscale structure of a multiplex can be organised via communities containing links in many different layers and, at the same time, communities having one predominant layer. This suggests that the mesoscale organization of multiplex networks has a rich mesoscale structure that is not captured by methods that aim at compressing the information on few single layers.

MATERIALS AND METHODS

Maximum Entropy Ensemble

To evaluate the similarity $S_{ik;jk}$ between two incident multilinks connecting nodes (i, k) and (j, k) we need to calculate the probability $p_{\ell_r}^{\vec{m}_{\ell_r}}$ of the multilinks \vec{m}_{ℓ_r} with $\ell = i, j$ and $r \neq k$ in our null model. The null model is a

maximum entropy ensemble determined by the probability $P(\vec{\mathcal{G}})$ associated to each possible multiplex network $\vec{\mathcal{G}}$ with adjacency matrices $\tilde{\mathbf{a}}^{[\alpha]}$ and satisfying the constraints

$$\sum_{\vec{\mathcal{G}}} \left(P(\vec{\mathcal{G}}) \sum_{r \neq k} \tilde{a}_{\ell r}^{[\alpha]} \right) = q_{\ell}^{[\alpha]} - a_{\ell k}^{[\alpha]}, \quad (9)$$

with $\alpha = 1, 2, \dots, M$, $\ell = i, j$ and $q_{\ell}^{[\alpha]}$ indicating the degree on node ℓ in layer α . (See SI for further details). Therefore the ensemble randomizes the original multiplex network by keeping constants the degrees $q_{\ell}^{[\alpha]}$ and the multilinks $\vec{m}_{\ell k}$ with $\ell = i, j$.

Link modularity

Let us consider the adjacency matrix \mathbf{W} determining the line graph of the aggregated network. This matrix has elements $W_{\ell, \ell'} = 1$ if the link ℓ is incident to the link ℓ' while otherwise $W_{\ell, \ell'} = 0$. For any given dendrogram cut, we indicate the cluster membership of multilink corresponding to the link ℓ of the aggregated network as c_{ℓ} . The link modularity \mathcal{Q} [26] is given by

$$\mathcal{Q} = \frac{1}{\sum_{\ell} d_{\ell}} \sum_{\ell, \ell'} \left[W_{\ell, \ell'} - \frac{d_{\ell} d_{\ell'}}{\sum_{\ell} d_{\ell}} \right] \delta(c_{\ell}, c_{\ell'}), \quad (10)$$

where $d_{\ell} = \sum_{\ell'} W_{\ell, \ell'}$ and $\delta(a, b) = 1$ if and only if $a = b$ otherwise $\delta(a, b) = 0$.

Codes

The codes implementing the Multilink Community detection method are freely available at the website: <https://github.com/ginestrab>.

Data

All the datasets analyzed in this paper are freely available on the data repository <http://deim.urv.cat/~manlio.dedomenico/data.php>.

ACKNOWLEDGMENTS

This research utilised Queen Mary's MidPlus computational facilities, supported by QMUL Research-IT and funded by EPSRC grant EP/K000128/1.

SUPPLEMENTARY INFORMATION

Supplementary Information on the Multilink Community detection algorithm

General considerations

The similarity between any two incident multilinks of the multiplex network is the basic element of the multilink community detection algorithm. The similarity matrix is used to perform a hierarchical clustering of the multilinks, ultimately finding the multilink communities as described in the main body of the paper. In the same spirit as in Ref. [33] the similarity matrix is constructed by comparing the local neighborhood of each pair of incident multilinks to a maximum entropy null model for the multiplex network.

Here we give further information on the maximum entropy null model that we used to evaluate the similarity between any two incident multilinks. This model extends previous results on exponential random graphs of single [37] and multiplex networks [3, 11].

Multiplex network

Let us consider a multiplex network $\vec{G} = \{G^{[1]}, G^{[2]}, \dots, G^{[\alpha]}, \dots, G^{[M]}\}$ formed by N nodes and M layers $\alpha = 1, 2, \dots, M$. Every layer α is formed by a undirected network with adjacency matrix $\mathbf{a}^{[\alpha]}$. Every pair of nodes (i, j) is connected by a multilink [3, 11]

$$\vec{m}_{ij} = \left(m_{ij}^{[1]}, m_{ij}^{[2]}, \dots, m_{ij}^{[\alpha]} \dots m_{ij}^{[M]} \right), \quad (\text{S-11})$$

with $m_{ij}^{[\alpha]} = a_{ij}^{[\alpha]}$ indicating in which layers of the multiplex network the two nodes are connected. Whenever node i and node j are connected at least in one layer, i.e. $\vec{m} \neq \vec{0}$, we say that they are connected by a non-trivial multilink.

The aggregated network \hat{G} is the single network in which any two nodes are connected if they are linked at least in one layer of the multiplex network. The adjacency matrix \mathbf{A} of the aggregated network \hat{G} has elements

$$A_{ij} = \theta \left(\sum_{\alpha=1}^M a_{ij}^{[\alpha]} \right), \quad (\text{S-12})$$

where $\theta(x)$ is the step function $\theta(x) = 1$ if $x > 0$ and $\theta(x) = 0$ if $x \leq 0$. We indicate with $L = \sum_{i < j} A_{ij}$ the total number of links of the aggregated network, or equivalently the number of non-trivial multilinks.

Multilink similarity

In order to detect the multilink communities we assign a non zero similarity $S_{ik,jk}$ to every pair of incident multilinks connecting respectively the generic nodes i and k and j and k . The non-zero similarities $S_{ik,jk}$ are given by

$$S_{ik,jk} = \epsilon \sigma_{ijk} + (1 - \epsilon) \sigma_{ij \setminus k}. \quad (\text{S-13})$$

where σ_{ijk} evaluates the contribution of the two incident multilinks while $\sigma_{ij \setminus k}$, evaluates instead the contribution due to the existence of other multilinks, joining node i and node j directly or by paths of length two excluding node k . The parameter $\epsilon \in (0, 1)$ tunes the relative importance between these two contributions. The term σ_{ijk} is expressed as

$$\sigma_{ijk} = z^{\beta_{ik,jk}}, \quad (\text{S-14})$$

with

$$\beta_{ij,rs} = 1 - \frac{\sum_{\alpha=1}^M m_{ij}^{[\alpha]} m_{rs}^{[\alpha]}}{M}. \quad (\text{S-15})$$

The term $\sigma_{ij \setminus k}$ includes contributions from paths of length one (\mathcal{M}_{ij}) and two ($\hat{\mathcal{M}}_{ijr}$) between node i and node j that pass through node r with $r \neq k$, i.e.

$$\sigma_{ij \setminus k} = \frac{1}{\mu} \left[\mathcal{M}_{ij} + \sum_{r \neq k} \hat{\mathcal{M}}_{ijr} \right], \quad (\text{S-16})$$

where μ is a normalization constant with $\mu = \max(1, \nu)$ with

$$\nu = \min \left(\sum_{r \neq k} A_{ir}, \sum_{r \neq k} A_{jr} \right). \quad (\text{S-17})$$

Similarly to the modularity measure [33], term \mathcal{M}_{ij} evaluates the significance of the observed multilink \vec{m}_{ij} against its expectation and, $\hat{\mathcal{M}}_{ijr}$ evaluates the significance of two non-trivial multilinks $\vec{m}_{ir}, \vec{m}_{jr}$ connecting respectively node i and node j to a common node $r \neq k$ against their expectations. These terms are

$$\begin{aligned} \mathcal{M}_{ij} &= (A_{ij} - p_{ij}^{\vec{m}_{ij}}) z^{\beta_{ij,ij}} \delta(A_{ij}, 1), \\ \hat{\mathcal{M}}_{ijr} &= (A_{ir} A_{jr} - p_{ir}^{\vec{m}_{ir}} p_{jr}^{\vec{m}_{jr}}) z^{\beta_{ir,jr}} \delta(A_{ir} A_{jr}, 1), \end{aligned} \quad (\text{S-18})$$

where $\beta_{ij,rs}$ is given by Eq. (S-15), and $\delta(x, y)$ is the Kronecker delta (i.e. $\delta(x, y) = 1$ for $x = y$ and $\delta(x, y) = 0$ otherwise). The expectation of multilink \vec{m}_{rs} is given by the probability $p_{rs}^{\vec{m}_{rs}}$, which is evaluated using maximum entropy ensembles.

The null model should not change the multilinks \vec{m}_{ik} and \vec{m}_{jk} determining the connection of nodes i and j with node k . This restriction fixes the connections between

node i and k and node j and k but it does not restrict the connections between nodes i and j and their other neighbors. To capture the local structure on layer α , the null model should preserve the number of neighbors of nodes i and j in each layer α , that is their degree $q_i^{[\alpha]}$ and $q_j^{[\alpha]}$, however, except from node k , the neighbors are selected at random from the remaining $N - 2$ nodes. Therefore the maximum entropy model is preserving the degree of node i and node j in each layer α , and the multilinks $\vec{m}_{ik}, \vec{m}_{jk}$.

Maximum entropy ensemble

The considered maximum entropy ensemble is characterised by the probability $P(\vec{\mathcal{G}})$ assigned to each possible multiplex network $\vec{\mathcal{G}}$ determined by the set of adjacency matrices $\vec{\mathbf{a}}^{[\alpha]}$ with $\alpha = 1, 2, \dots, M$. This probability is found by maximising the entropy S which is the logarithm of the number of typical multiplex networks in the ensemble,

$$S = - \sum_{\vec{\mathcal{G}}} P(\vec{\mathcal{G}}) \ln P(\vec{\mathcal{G}}) \quad (\text{S-19})$$

given the set of structural constraints under consideration. These constraints are

$$\begin{aligned} \sum_{\vec{\mathcal{G}}} \left(P(\vec{\mathcal{G}}) \sum_{r \neq k} \tilde{a}_{ir}^{[\alpha]} \right) &= q_i^{[\alpha]} - a_{ik}^{[\alpha]}, \\ \sum_{\vec{\mathcal{G}}} \left(P(\vec{\mathcal{G}}) \sum_{r \neq k} \tilde{a}_{jr}^{[\alpha]} \right) &= q_j^{[\alpha]} - a_{jk}^{[\alpha]}, \end{aligned} \quad (\text{S-20})$$

with $\alpha = 1, 2, \dots, M$. By introducing the Lagrangian multipliers $\lambda_i^{[\alpha]}, \lambda_j^{[\alpha]}$ with $\alpha = 1, 2, \dots, M$ the probability $P(\vec{\mathcal{G}})$ can be written as

$$P(\vec{\mathcal{G}}) = \frac{1}{Z} e^{-\sum_{\alpha=1}^M H_{ij}^{[\alpha]}}, \quad (\text{S-21})$$

where the partition function Z is a normalization constant, and $H_{ij}^{[\alpha]}$ is given by

$$\begin{aligned} H_{ij}^{[\alpha]} &= \lambda_i^{[\alpha]} \left(\sum_{r \neq \{k, i, j\}} \tilde{a}_{ir}^{[\alpha]} \right) + \lambda_j^{[\alpha]} \left(\sum_{r \neq \{k, i, j\}} \tilde{a}_{jr}^{[\alpha]} \right) \\ &\quad + (\lambda_i^{[\alpha]} + \lambda_j^{[\alpha]}) \tilde{a}_{ij}^{[\alpha]}. \end{aligned} \quad (\text{S-22})$$

The marginal probability of single links of nodes i and node j in each layer α are given, for $r \neq \{i, j, k\}$ by

$$\begin{aligned} p_{ir}^{[\alpha]} &= \sum_{\vec{\mathcal{G}}} \left(P(\vec{\mathcal{G}}) \tilde{a}_{ir} \right) = \frac{e^{-\lambda_i^{[\alpha]}}}{1 + e^{-\lambda_i^{[\alpha]}}}, \\ p_{jr}^{[\alpha]} &= \sum_{\vec{\mathcal{G}}} \left(P(\vec{\mathcal{G}}) \tilde{a}_{jr} \right) = \frac{e^{-\lambda_j^{[\alpha]}}}{1 + e^{-\lambda_j^{[\alpha]}}}, \end{aligned} \quad (\text{S-23})$$

and by

$$p_{ij}^{[\alpha]} = \sum_{\vec{G}} \left(P(\vec{G}) \tilde{a}_{ij} \right) = \frac{e^{-\lambda_i^{[\alpha]} - \lambda_j^{[\alpha]}}}{1 + e^{-\lambda_i^{[\alpha]} - \lambda_j^{[\alpha]}}}. \quad (\text{S-24})$$

The Lagrangian multipliers $\lambda_i^{[\alpha]}$ and $\lambda_j^{[\alpha]}$ are determined by the constraints in Eq. (S-20) that, in terms of the marginals is

$$\begin{aligned} \left(\sum_{r \neq \{j,k\}} p_{ir}^{[\alpha]} \right) + p_{ij}^{[\alpha]} &= q_i^{[\alpha]} - a_{ik}^{[\alpha]}, \\ \left(\sum_{r \neq \{i,k\}} p_{jr}^{[\alpha]} \right) + p_{ij}^{[\alpha]} &= q_j^{[\alpha]} - a_{jk}^{[\alpha]}. \end{aligned} \quad (\text{S-25})$$

Finally this maximum entropy ensemble allow us to determine the probability $p_{ir}^{\vec{m}_{ir}}$ and $p_{jr}^{\vec{m}_{jr}}$ of the multilinks $\vec{m}_{ir}, \vec{m}_{jr}$ which are given respectively by

$$\begin{aligned} p_{ir}^{\vec{m}_{ir}} &= \sum_{\vec{G}} P(\vec{G}) \prod_{\alpha=1}^M \left(\tilde{a}_{ir}^{[\alpha]} m_{ir}^{[\alpha]} + (1 - \tilde{a}_{ir}^{[\alpha]})(1 - p_{ir}^{[\alpha]}) \right) \\ &= \prod_{\alpha=1}^M \left(p_{ir}^{[\alpha]} m_{ir}^{[\alpha]} + (1 - m_{ir}^{[\alpha]})(1 - p_{ir}^{[\alpha]}) \right), \end{aligned} \quad (\text{S-26})$$

and

$$\begin{aligned} p_{jr}^{\vec{m}_{jr}} &= \sum_{\vec{G}} P(\vec{G}) \prod_{\alpha=1}^M \left(\tilde{a}_{jr}^{[\alpha]} m_{jr}^{[\alpha]} + (1 - \tilde{a}_{jr}^{[\alpha]})(1 - p_{jr}^{[\alpha]}) \right) \\ &= \prod_{\alpha=1}^M \left(p_{jr}^{[\alpha]} m_{jr}^{[\alpha]} + (1 - m_{jr}^{[\alpha]})(1 - p_{jr}^{[\alpha]}) \right). \end{aligned} \quad (\text{S-27})$$

Multilink communities

From the $L \times L$ similarity matrix $S_{ik,js}$, we construct a dendrogram via single linkage hierarchical clustering. The multilink communities are obtained by cutting the dendrogram at a height that correspond to the maximum value of the link modularity \mathcal{Q} .

The link modularity \mathcal{Q} [26] is given by

$$\mathcal{Q} = \frac{1}{\sum_{\ell} d_{\ell}} \sum_{\ell, \ell'} \left[W_{\ell, \ell'} - \frac{d_{\ell} d_{\ell'}}{\sum_{\ell} d_{\ell}} \right] \delta(c_{\ell}, c_{\ell'}), \quad (\text{S-28})$$

where \mathbf{W} is the adjacency matrix of the line graph of the aggregated network and has elements $W_{\ell, \ell'} = 1$ if the link ℓ is incident to the link ℓ' while otherwise $W_{\ell, \ell'} = 0$. Additionally in Eq. (S-28) we indicate with d_{ℓ} the link-degree $d_{\ell} = \sum_{\ell'} W_{\ell, \ell'}$ and with c_{ℓ} the cluster membership of the multilink corresponding to the link ℓ of the aggregated network. Finally $\delta(a, b) = 1$ if and only if $a = b$ otherwise $\delta(a, b) = 0$.

Once every multilink is associated to a given multilink community, each node is attributed a *community activity* given by the number of different communities to which its incident multilinks belong.

Supplementary Information on the results obtained on real datasets with the Multilink Community detection algorithm

More on the benchmark multiplex network

As mentioned in the main part of the paper when considering the example of the simple multiplex shown in Fig. 1(a)-(b). The right and left multilink communities have a different internal structure due to a subtle factor, this difference is clearly seen in the dendrogram Fig. 1(b). To explain this difference we consider a very simple multiplex. Figure S-6(a) shows this simple multiplex network and its partition into multilink communities (shaded areas). Although the community structure of this multiplex network is identical to Fig. 1(c), its dendrogram (Fig. S-6(b)) is again, not symmetric under the permutation of the right and left communities. The difference is due to the multiplexity of the network. In fact node f and node d play slightly different roles in their communities. Node f is active in two different layers, while node d is active only in one layer. Our method distinguishes these two cases.

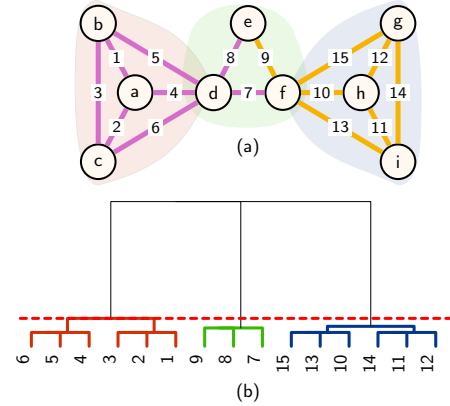


FIG. S-6: (a) A simple two layer multiplex network (purple and ochre links) and its multilink communities (shaded areas) and (b) its dendrogram obtained from the multilink similarity. The dashed red line shows the maximum link modularity used to define the link communities.

Aggregated degree vs. community activity

We investigated if there is a correlation between the degree of the aggregated network \hat{G} and the community activity of the nodes. Figure S-9 shows community activity vs. degree of the aggregated network for the Multiplex Connectome of *C. elegans* (Fig. S-9(a)) and the European Multiplex Air Transportation Network (Fig. S-9(b)). For small degrees, there is a significant positive correlation

between these two quantities, but as the degree increases, the correlation diminishes.

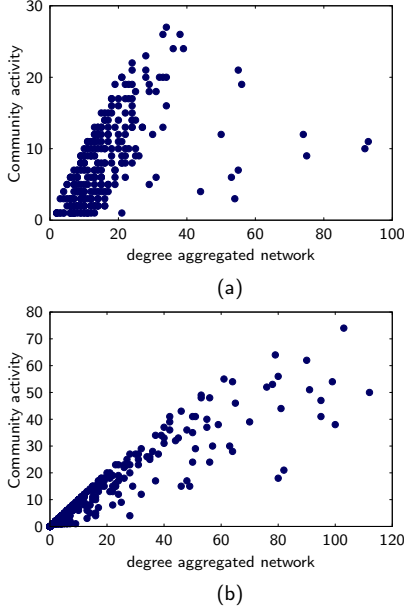


FIG. S-7: Aggregated degree vs. community activity for the (a) Multiplex Connectome of *C. elegans* and (b) for the European Multiplex Air Transportation Network.

The score function profile of the analyzed datasets

The multilink communities are determined by cutting the dendrogram at a height that corresponds to the maximum value of the score function Q . In the datasets considered here, we observed that the profile of the link modularity Q (Fig. S-8) displays a well defined global maximum, suggesting that the determination of the optimal partition is not questionable.

The number of multilink communities as a function of the parameters ϵ and z

In general the values of the parameters z and ϵ will depend on the network under consideration. The parameters used in the here were chosen to demonstrate the dependence of the number of multilink communities

as function of the parameters. An example of this dependence is shown in Fig. S-9(a)-(b) for the Florentine families. We noticed that for many different values of the parameters the method consistently divided the multiplex into five link communities, in the manuscript we used $\epsilon = 0.4$ and $z = 0.6$ to show these five link communities.

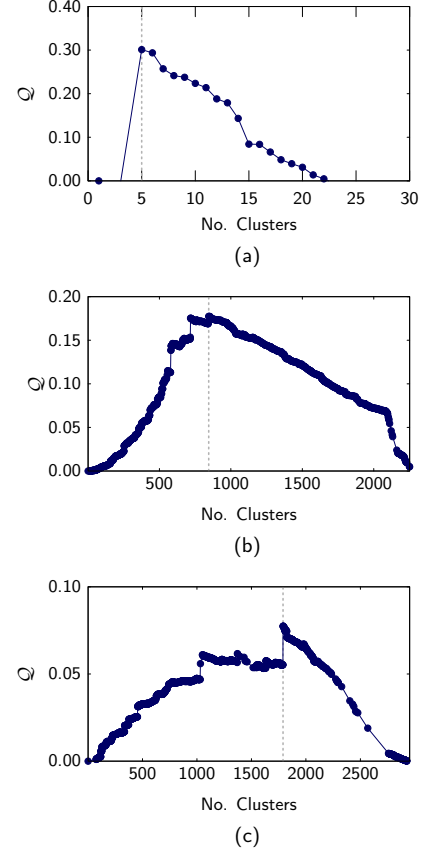


FIG. S-8: Number of clusters against the score function Q (link-modularity) for the (a) Florentine Families Multiplex Network ($\epsilon = 0.5, z = 0.6$), (b) for the Multiplex Connectome of *C. elegans* ($\epsilon = 0.4, z = 0.6$) and (c) for the European Multiplex Air Transportation Network ($\epsilon = 0.4, z = 0.6$). The maximum of Q determines the number of clusters which define the multilink communities of the multiplex network.

[1] Stefano Boccaletti, Ginestra Bianconi, Regino Criado, Charo I Del Genio, Jesús Gómez-Gardenes, Miguel Romance, Irene Sendina-Nadal, Zhen Wang, and Massimiliano Zanin. The structure and dynamics of multilayer networks. *Physics Reports*, 544(1):1–122, 2014.

[2] Mikko Kivelä, Alex Arenas, Marc Barthélemy, James P Gleeson, Yamir Moreno, and Mason A Porter. Multilayer networks. *Journal of complex networks*, 2(3):203–271, 2014.

[3] Ginestra Bianconi. Statistical mechanics of multiplex

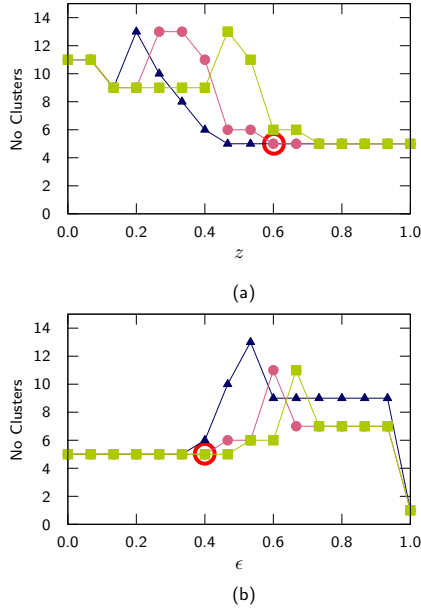


FIG. S-9: (a) Variation of the number of clusters for the Florentine families multiplex as a function of z where the data shown are for $\epsilon = 0.4$ (blue triangles), $\epsilon = 0.5$ (pink circles) and $\epsilon = 0.6$ (green squares). (b) Variation of the number of clusters for the Florentine families multiplex as a function of ϵ where the data shown are for $z = 0.4$ (blue triangles), $z = 0.5$ (pink circles) and $z = 0.6$ (green squares). In both figures the red circle marks the values of the parameters used in Fig. 2

networks: Entropy and overlap. *Physical Review E*, 87(6):062806, 2013.

- [4] Sergey V Buldyrev, Roni Parshani, Gerald Paul, H Eugene Stanley, and Shlomo Havlin. Catastrophic cascade of failures in interdependent networks. *Nature*, 464(7291):1025–1028, 2010.
- [5] Sergio Gomez, Albert Diaz-Guilera, Jesus Gomez-Gardenes, Conrad J Perez-Vicente, Yamir Moreno, and Alex Arenas. Diffusion dynamics on multiplex networks. *Physical review letters*, 110(2):028701, 2013.
- [6] Jia Shao, Sergey V Buldyrev, Shlomo Havlin, and H Eugene Stanley. Cascade of failures in coupled network systems with multiple support-dependence relations. *Physical Review E*, 83(3):036116, 2011.
- [7] Xuqing Huang, Jianxi Gao, Sergey V Buldyrev, Shlomo Havlin, and H Eugene Stanley. Robustness of interdependent networks under targeted attack. *Physical Review E*, 83(6):065101, 2011.
- [8] Vincenzo Nicosia and Vito Latora. Measuring and modeling correlations in multiplex networks. *Physical Review E*, 92(3):032805, 2015.
- [9] Peter J Mucha, Thomas Richardson, Kevin Macon, Mason A Porter, and Jukka-Pekka Onnela. Community structure in time-dependent, multiscale, and multiplex networks. *Science*, 328(5980):876–878, 2010.
- [10] Michael Szell, Renaud Lambiotte, and Stefan Thurner. Multirelational organization of large-scale social networks in an online world. *Proceedings of the National Academy of Sciences*, 107(31):13636–13641, 2010.
- [11] Giulia Menichetti, Daniel Remondini, Pietro Panzarasa, Raúl J Mondragón, and Ginestra Bianconi. Weighted multiplex networks. *PloS one*, 9(6):e97857, 2014.
- [12] Barry Bentley, Robyn Branicky, Christopher L Barnes, Yee Lian Chew, Eviatar Yemini, Edward T Bullmore, Petra E Vértés, and William R Schafer. The multilayer connectome of caenorhabditis elegans. *PLOS Computational Biology*, 12(12):e1005283, 2016.
- [13] Manlio De Domenico, Albert Solé-Ribalta, Sergio Gómez, and Alex Arenas. Navigability of interconnected networks under random failures. *Proceedings of the National Academy of Sciences*, 111(23):8351–8356, 2014.
- [14] Alessio Cardillo, Jesús Gómez-Gardenes, Massimiliano Zanin, Miguel Romance, David Papo, Francisco Del Pozo, and Stefano Boccaletti. Emergence of network features from multiplexity. *Scientific reports*, 3:1344, 2013.
- [15] Federico Battiston, Jacopo Iacovacci, Vincenzo Nicosia, Ginestra Bianconi, and Vito Latora. Emergence of multiplex communities in collaboration networks. *PloS one*, 11(1):e0147451, 2016.
- [16] Jacopo Iacovacci, Zhihao Wu, and Ginestra Bianconi. Mesoscopic structures reveal the network between the layers of multiplex data sets. *Physical Review E*, 92(4):042806, 2015.
- [17] Ta-Chu Kao and Mason A Porter. Layer communities in multiplex networks. *arXiv preprint arXiv:1706.04147*, 2017.
- [18] Manlio De Domenico, Andrea Lancichinetti, Alex Arenas, and Martin Rosvall. Identifying modular flows on multilayer networks reveals highly overlapping organization in interconnected systems. *Physical Review X*, 5(1):011027, 2015.
- [19] Lucas GS Jeub, Michael W Mahoney, Peter J Mucha, and Mason A Porter. A local perspective on community structure in multilayer networks. *Network Science*, pages 1–20, 2017.
- [20] Laura Bennett, Aristotelis Kittas, Gareth Muirhead, Lazaros G Papageorgiou, and Sophia Tsoka. Detection of composite communities in multiplex biological networks. *Scientific reports*, 5:10345, 2015.
- [21] Zhana Kuncheva and Giovanni Montana. Community detection in multiplex networks using locally adaptive random walks. In *Proceedings of the 2015 IEEE/ACM International Conference on Advances in Social Networks Analysis and Mining 2015*, pages 1308–1315. ACM, 2015.
- [22] Andrea Lancichinetti and Santo Fortunato. Consensus clustering in complex networks. *Scientific reports*, 2, 2012.
- [23] Santo Fortunato and Darko Hric. Community detection in networks: A user guide. *Physics Reports*, 659:1–44, 2016.
- [24] Michael T Schaub, Jean-Charles Delvenne, Martin Rosvall, and Renaud Lambiotte. The many facets of community detection in complex networks. *arXiv preprint arXiv:1611.07769*, 2016.
- [25] Yong-Yeol Ahn, James P Bagrow, and Sune Lehmann. Link communities reveal multiscale complexity in networks. *Nature*, 466(7307):761–764, 2010.
- [26] TS Evans and R Lambiotte. Line graphs, link partitions, and overlapping communities. *Physical Review E*, 80(1):016105, 2009.
- [27] Gergely Palla, Imre Derényi, Illés Farkas, and Tamás

- Vicsek. Uncovering the overlapping community structure of complex networks in nature and society. *Nature*, 435(7043):814–818, 2005.
- [28] Manlio De Domenico, Vincenzo Nicosia, Alexandre Arenas, and Vito Latora. Structural reducibility of multilayer networks. *Nature communications*, 6, 2015.
- [29] Toni Valles-Catala, Francesco A Massucci, Roger Guimera, and Marta Sales-Pardo. Multilayer stochastic block models reveal the multilayer structure of complex networks. *Physical Review X*, 6(1):011036, 2016.
- [30] Tiago P Peixoto. Inferring the mesoscale structure of layered, edge-valued, and time-varying networks. *Physical Review E*, 92(4):042807, 2015.
- [31] Davide Cellai and Ginestra Bianconi. Multiplex networks with heterogeneous activities of the nodes. *Physical Review E*, 93(3):032302, 2016.
- [32] Erzsébet Ravasz and Albert-László Barabási. Hierarchical organization in complex networks. *Physical Review E*, 67(2):026112, 2003.
- [33] Mark EJ Newman. Modularity and community structure in networks. *Proceedings of the national academy of sciences*, 103(23):8577–8582, 2006.
- [34] John F Padgett and Christopher K Ansell. Robust action and the rise of the medici, 1400-1434. *American journal of sociology*, 98(6):1259–1319, 1993.
- [35] Beth L Chen, David H Hall, and Dmitri B Chklovskii. Wiring optimization can relate neuronal structure and function. *Proceedings of the National Academy of Sciences of the United States of America*, 103(12):4723–4728, 2006.
- [36] Manlio De Domenico, Mason A Porter, and Alex Arenas. Muxviz: a tool for multilayer analysis and visualization of networks. *Journal of Complex Networks*, page cnu038, 2014.
- [37] Juyong Park and Mark EJ Newman. Statistical mechanics of networks. *Physical Review E*, 70(6):066117, 2004.